Vascular brassinosteroid receptors confer drought resistance without penalizing plant growth

Norma Fàbregas[1,*], Fidel Lozano-Elena[1,*], David Blasco-Escámez[1], Takayuki Tohge[2,8], Cristina Martínez-Andújar[3], Alfonso Albacete[3], Sonia Osorio[4], Mariana Bustamante[1], José Luis Riechmann[1,9], Takahito Nomura[5], Takao Yokota[6], Ana Conesa[7] , Francisco Pérez Alfocea[3], Alisdair R. Fernie[2] and Ana I. Caño-Delgado[1,¶]

[1]*Centre for Research in Agricultural Genomics (CRAG) CSIC-IRTA-UAB-UB, Barcelona 08193, Spain.*

[2]*Max Planck Institute of Molecular Plant Physiology, Potsdam-Golm D-14476, Germany.*

[3]*Department of Plant Nutrition, CEBAS-CSIC, Murcia 30100, Spain.*

[4]*Instituto de Hortofruticultura Subtropical y Mediterránea "La Mayora". University of Málaga-Consejo Superior de Investigaciones Científicas. Department of Molecular Biology and Biochemistry, Málaga 29071, Spain.*

[5]*Center for Bioscience Research and Education, Utsunomiya University, Minemachi, Utsunomiya 321-8505, Japan.*

[6]*Department of Biosciences, Teikyo University,Toyosatodai, Utsunomiya 320-8551, Japan.*

[7]*Microbiology and Cell Science Department, IFAS, Genetics Institute, University of Florida, Gainesville 32603, USA.*

[8]*Current Address: NAIST Graduate school of Biological Sciences, 8916-5 Takayama, Ikoma, Nara 630-0192, Japan.*

[9]*Institució Catalana de Recerca i Estudis Avançats (ICREA), Barcelona, 08010, Spain*

[*] Both authors contributed equally to this work.

[¶] Correspondence to: ana.cano@cragenomica.es

ABSTRACT

Drought represents a major threat to food security. Mechanistic data describing plant responses to drought have been studied extensively and genes conferring drought resistance have been introduced into crop plants. However, plants with enhanced drought resistance usually display lower growth, highlighting the need for strategies to uncouple drought resistance from growth. Here, we show that overexpression of BRL3, a vascular-enriched member of the brassinosteroid receptor family, can confer drought stress in Arabidopsis. Whereas loss-of-function mutations in the ubiquitously expressed BRI1 receptor leads to drought resistance at the expense of growth, overexpression of BRL3 receptor confers drought tolerance without penalizing overall growth. Systematic analyses reveal that upon drought stress, increased BRL3 triggers the accumulation of osmoprotectant metabolites including proline and sugars. Transcriptomic analysis suggests that this results from differential expression of genes in the vascular tissues. Altogether, this data suggests that manipulating BRL3 expression could be used to engineer drought tolerant crops.

50 **INTRODUCTION**

51 Drought is responsible for at least 40% of crop losses worldwide and this
52 proportion is dramatically increasing due to climate change [1]. Understanding
53 cellular responses to drought stress represents the first step toward the
54 development of better-adapted crops, something which is a great challenge for
55 the field of plant biotechnology [2]. Classical approaches aimed at examining how
56 plants cope with limited water led to the identification of regulators involved in
57 the signal transduction cascades of the abscisic acid (ABA)-dependent and
58 ABA-independent pathways [3]. Adaptation to drought stress has been
59 associated with the presence of proteins that protect cells from dehydration,
60 such as late-embryogenesis–abundant (LEA) proteins, osmoprotectants and
61 detoxification enzymes [4,5]. These studies provided deep insights into the
62 molecular mechanisms underlying abiotic stress [2], showing that drought
63 resistance is a complex trait simultaneously controlled by many genes. While
64 genetic approaches have succeeded in conferring stress resistance to plants,
65 this generally comes at the cost of reduced growth [6,7]. Therefore, understanding
66 how cellular growth is coupled to drought stress responses is essential for
67 engineering plants with improved growth in rainfed environments.

68 Receptor-like kinases (RLKs) play an important role in optimizing plant
69 responses to stress [8,9]. Brassinosteroid (BR) hormones directly bind to BRI1
70 (BR-INSENSITIVE 1) leucine-rich repeat (LRR)-RLK family members on the
71 plasma membrane [10-14]. Ligand perception triggers BRI1 to interact with the co-
72 receptor BAK1 (BRI1 ASSOCIATED RECEPTOR KINASE 1) [15-17], which is
73 essential for early BR signaling events [18]. This BRI1-BAK1 heterodimerization
74 initiates a signaling cascade of phosphorylation events that control the

75 expression of multiple BR-regulated genes mainly via the BRI1-EMS-
76 SUPPRESSOR1 (BES1) and BRASSINAZOLE RESISTANT1 (BZR1)
77 transcription factors [19-21].
78 Although BRs modulate multiple developmental and environmental stress
79 responses in plants, the exact role of BRs under stress conditions remains
80 controversial. Whereas the exogenous application of BRs and the
81 overexpression of the BR biosynthetic enzyme DWF4 both confer increased
82 plant adaptation to drought stress [22-24], suppression of the BRI1 receptor also
83 results in drought-resistant phenotypes [25,26]. Intriguingly, ABA signaling inhibits
84 the BR signaling pathway after BR perception, and crosstalk between the two
85 pathways upstream of the BIN2 (BRASSINOSTEROID-INSENSITIVE 2) kinase
86 has been reported [27,28]. Further crosstalk has been described downstream
87 mediated by the overlapping transcriptional control of multiple BR- and ABA-
88 regulated genes [29,30] such as *RESPONSE TO DESICCATION 26* (*RD26*) [26].
89 Recently, greater attention is being placed on the spatial regulation of hormonal
90 signaling pathways in attempt to further understand the coordination of plant
91 growth and stress responses [26,31-34]. For instance, while the BRI1 receptor is
92 widely localized in many tissues [35], the BRI1-LIKE receptor homologues BRL1
93 and BRL3 signal from the innermost tissues of the plant and thereby contribute
94 to vascular development [12,33,36]. BR receptor complexes are formed by different
95 combinations of BRI1-like LRR-RLKs with the BAK1 co-receptor in the plasma
96 membrane [33]. Despite BRI1 being a central player in plant growth and
97 adaptation to abiotic stress [26,37,38], the functional relevance of vascular BRL1 and
98 BRL3 is only just beginning to be explored [33,39]. For example, in previous
99 proteomic approaches we found abiotic stress-related proteins within BRL3

100 signalosome complexes [33], but the exact role of the BRL3 pathway in drought
101 remains elusive.
102 Here, we show that the different BR receptors modulate a plant´s adaptive
103 response to multiple drought stress traits in both the roots and shoots. While the
104 traits controlled by the BRI1 pathway are intimately linked to growth arrest, we
105 found that increased levels of vascular-enriched BRL3 receptors confer drought
106 resistance without penalizing overall plant growth. Moreover, metabolite
107 profiling revealed that the overexpression of the BRL3 receptor triggers the
108 production of an osmoprotectant signature (i.e., proline, trehalose, sucrose, and
109 raffinose family oligosaccharides) in the plant and the specific accumulation of
110 the osmoprotectant metabolites in the roots during periods of drought.
111 Subsequent transcriptomic profiling showed that this metabolite signature is
112 transcriptionally regulated by the BRL3 pathway in response to drought. An
113 enrichment of deregulated genes in root vascular tissues, especially in the
114 phloem, further supports a preferential accumulation of osmoprotectant
115 metabolites to the root. Overall, this study demonstrates that overexpression of
116 the BRL3 receptor boosts the accumulation of sugar and osmoprotectant
117 metabolites in the root to overcome drought-associated growth arrest, thereby
118 uncovering a strategy to protect crops against drought.
119
120 **RESULTS**
121 **BR receptors control osmotic stress sensitivity in the root**
122 To determine the contribution of the BR complexes in the response to drought,
123 we performed a comprehensive characterization of different combinations of
124 mutants of all the BR receptors and the BAK1 co-receptor. For each

125 combination, we first analyzed primary root growth (Fig. 1a). As previously
126 described [17,33,40], seven-day-old roots of *bak1*, *brl1brl3bak1*, *bri1*, and
127 *bri1brl1brl3* displayed shorter roots than the Col-0 wild type (WT). We also
128 found that the primary roots of the quadruple mutant *bri1brl1brl3bak1* (hereafter
129 *quad*) were the shortest and the most insensitive to BRs (Fig. 1a,b and
130 Supplementary Fig. 1). Conversely, plants overexpressing BRL3 (*35S:BRL3-*
131 *GFP,* hereafter *BRL3ox*) not only exhibited longer roots than WT (Fig. 1a,b) but
132 also showed increased receptor levels in root vascular tissues [33]
133 (Supplementary Fig. 2). These results agree with the previously reported role of
134 BR receptors in promoting root growth [40,41]. We then subjected Arabidopsis
135 seedlings to osmotic stress by transferring them to sorbitol-containing media
136 and subsequently quantified the level of inhibition of root growth in sorbitol
137 relative to control conditions (see Methods). A significantly lower level of relative
138 root growth inhibition mediated by osmotic stress was observed in *bri1* (27%),
139 *bri1brl1brl3* (28%) and *quad* (27%) mutants compared to the WT (39%; Fig.
140 1a,b). In contrast, no differences were found in *brlbrl3* and *brl1brl3bak1* root
141 growth inhibition when compared to WT (Fig. 1a,b). Similarly, the roots of
142 *BRL3ox* plants were like those of WT in terms of relative root growth inhibition
143 (Fig. 1a,b).
144 Previous experimental evidences unveiled that the water stress-induced cell
145 death in Arabidopsis roots is localized and undergoes programmed cell death
146 (PCD) [42]. As shown by the incorporation of propidium iodine (PI) into the nuclei
147 (Fig. 1c,d), a short period of osmotic stress (24h) caused cell death in the
148 elongation zone of WT roots. In comparison, a reduced amount of cell death
149 was observed in the roots of *bri1, bri1brl1brl3* and *quad* mutants (Fig. 1c,d),

150 thereby indicating less sensitivity towards osmotic stress. Conversely, plants
151 with increased levels of BRL3 receptor showed a massive amount of cell death
152 in the root tips compared to the WT, indicating an increased sensitivity to short
153 osmotic stress (Fig 1c,d). These results point towards a role for BR receptors in
154 triggering osmotic stress responses in the plant root.
155 Since root hydrotropism represents a key feature for adaptation to environments
156 scarce in water [43], we investigated the capacity of roots to escape imposed
157 osmotic stress by bending towards water-available media (Fig. 2a). We found
158 that BR receptors loss-of-function mutants had reduced hydrotropic responses
159 compared to WT plants. For instance, while no significant differences were
160 found under control conditions (mock) (Supplementary Fig. 3), the roots of BR
161 receptor mutants grew straighter than WT roots towards the sorbitol-containing
162 media (Fig. 2a-c). Interestingly, *brl1brl3bak1* mutants were the most insensitive
163 to osmotic stress in terms of hydrotropism, showing lower root curvature angles
164 than the *quad* roots (Fig. 2b). Consistently, compared to WT roots, an enhanced
165 hydrotropic response was observed in *BRL3ox* (Fig. 2a-c). Furthermore,
166 exogenous application of the BR synthesis inhibitor brassinazole [44] reverted the
167 hydrotropic response of WT roots (Supplementary Fig. 3). For better
168 visualization, we generated a drought multi-trait matrix for all the BR receptor
169 mutants analyzed in this study (Fig. 2d; Supplementary Table 1). From this
170 matrix, it can be seen that the BRL3/BRL1/BAK1 receptors in the vascular
171 tissues enhances hydrotropic sensitivity.
172
173 ***BRL3ox* confers drought resistance without penalizing growth**

174 To investigate if the impaired responses to abiotic stress observed in root
175 seedling were preserved in mature plants, we next analyzed the phenotypes of
176 plants exposed to severe drought. After 12 days of withholding water, dramatic
177 symptoms of drought stress were observed in WT, *brl1brl3* and *brl1brl3bak1*
178 mutants. In contrast, other BR mutants showed a remarkable degree of drought
179 resistance. In particular, *bak1*, *bri1*, *bri1brl1brl3*, and *quad* mutant plants were
180 the most resistant to the severe water-withholding regime (Fig. 3a). As these
181 mutants exhibited some degree of dwarfism (Fig. 3a), we confirmed their
182 resistance to drought by examining their survival rates after re-watering (Fig.
183 3b). To correct for the delayed growth seen in BR-deficient mutants, plants were
184 submitted to a time course of drought stress in which water use, photosynthesis
185 and transpiration parameters were monitored under similar relative soil water
186 content (Fig. 3c-e). The WT plants took just 9 days to use 70% of the available
187 water (field capacity) during the drought period (Fig. 3c). In comparison, BR
188 loss-of-function mutant plants *bri1*, *bri1brl1brl3* and *quad* took 15 days. All
189 subsequent measurements were done at the same soil water content for each
190 genotype. We found that the relative water content (RWC) in WT plants was
191 reduced during drought, while RWC in BR mutant leaves remained as in well-
192 watered conditions (Fig. 3d). In addition, compared to WT plants, BR mutants
193 sustained higher levels of photosynthesis and transpiration during the drought
194 period (Fig. 3e and Supplementary Fig. 4). Altogether our results indicate that
195 the dwarf BR receptor mutant plants are more resistant while consuming less
196 water, likely through avoiding the effects of drought (Fig. 3f).
197 Strikingly, we found that *BRL3ox* plants were more resistant than WT plants to
198 severe drought stress as shown by increased survival rates (Fig. 3a,b). Plants

199 with increased BRL3 receptors showed reduction of RWC during drought
200 similarly to WT plants (Fig. 3d). Interestingly the rate of photosynthesis was
201 lower in *BRL3ox* compared to WT at basal conditions, but together with
202 transpiration, was more stable than in WT plants during the drought period (Fig.
203 3,e and Supplementary Fig. 4). This indicates that *BRL3ox* plants are healthier
204 than WT under the same water consumption conditions. These results suggest
205 that the BRL3 pathway actively promotes drought tolerance without penalizing
206 plant growth (Fig. 3f).
207
208 **BRL3 triggers the production of osmoprotectant metabolites**
209 To further investigate the cause behind BRL3 receptor-conferred drought
210 tolerance, we performed metabolite profiling of *BRL3ox* plants and compared it
211 to the profile of WT and *quad* plants in a time course drought experiment. Roots
212 were separated from shoots to address possible changes in metabolite
213 accumulation from source to sink tissues. The complete metabolic fingerprints
214 are provided in Supplementary Fig. 5 and 6 and Supplementary Data 1 and 2.
215 Metabolite profiling of mature *BRL3ox* plants grown in control conditions (time
216 0) revealed an increment in the production of osmoprotectant metabolites. Both
217 shoots (Fig. 4a) and roots (Fig. 4b) of the *BRL3ox* plants exhibited metabolic
218 signatures enriched in proline and sugars, metabolites which have previously
219 been reported to confer resistance to drought [45-47]. This suggests that the BRL3
220 receptor promotes priming [48]. Importantly, the levels of these metabolites were
221 lower in *quad* mutant plants (Fig. 4a,c).
222 Compared to in WT, sugars including fructose, glucose, galactinol, galactose,
223 maltose, and raffinose were accumulated in the shoots of *BRL3ox* (Fig. 4a).

224 Conversely, whereas glucose levels were lower in the roots, sucrose, trehalose,
225 *myo*-inositol, and maltose appeared to accumulate here (Fig. 4b) suggesting
226 that the BRL3 pathway promotes sugar accumulation preferentially in the roots.
227 We then analyzed the dynamics of each metabolite in response to drought (see
228 Methods). In this time course, a rapid accumulation of osmoprotectant
229 metabolites was observed in *BRL3ox* plants (Fig. 4c,d). In the shoots, proline
230 showed the highest levels respect WT along the entire drought time course (Fig.
231 4c,f). In contrast, glucose, galactose and *myo*-inositol increased at similar or
232 slightly lower rates than in the shoots of WT plant (Fig. 4c,e,g). However, in
233 roots, an accumulation of trehalose, sucrose, proline, and raffinose was
234 observed in *BRL3ox* mutants subjected to drought stress (Fig. 4d), and this
235 accumulation showed steeper exponential dynamics than in WT plants (Fig.
236 4h). Additionally, glucose, galactose, fructose, and *myo*-inositol linearly
237 increased in WT roots but exponentially increased in *BRL3ox* roots (Fig. 4j).
238 Interestingly, throughout this time course, the levels of these metabolites were
239 lower in the *quad* mutant plants compared to in WT (Supplementary Fig. 7).
240 Altogether, these findings uncover a key role for BR receptors in promoting
241 sugar metabolism, and support the idea that BRL3 triggers the accumulation of
242 osmoprotectant metabolites in the root to promote growth during periods of
243 drought.
244
245 **BRL3 transcriptionally controls the drought metabolic response**
246 The accumulation of osmolytes in the roots of plants with increased levels of
247 BRL3 suggests faster sugar mobilization from shoots to roots. Thus, we next
248 investigated whether these metabolic pathways are transcriptionally regulated

249 by BRL3 in the root. RNAseq of *BRL3ox* roots revealed 759 deregulated genes
250 at basal conditions (214 upregulated and 545 downregulated; FC>1.5,
251 FDR<0.05; Supplementary Data 3) and 1,068 deregulated genes in drought
252 conditions (378 upregulated and 690 downregulated; FC>1.5, FDR<0.05;
253 Supplementary Data 4). In control conditions, a high proportion of the
254 deregulated genes belonged to the response to water stress, oxygen-containing
255 compounds (ROS) and response to ABA GO categories (Fig. 5a, 5c,
256 Supplementary Data 5 and 6). We next deployed the genes falling into the
257 response to stress category, which included classical drought stress markers
258 such as *RD22* and *RAB18* that were already upregulated in basal conditions
259 (Fig 5b). An enrichment of genes belonging to the response to hormone
260 category indicated altered hormonal responses in *BRL3ox* plants under drought
261 (Fig 5a,c and Supplementary Data 7 and 8). Further analyses of specific
262 hormonal responses revealed that the ABA and jasmonic acid (JA) were the
263 most altered responses (Supplementary Fig. 8). Repression of JA biosynthesis
264 genes resulted in decreased levels of JA in basal conditions (Supplementary
265 Fig. 8).
266 In order to uncover differential drought responses between WT and *BRL3ox*
267 roots, we constructed a linear model accounting for the interaction between
268 genotype and drought (Supplementary Data 9). Taking the 200 most
269 significantly affected genes, we grouped them in (i) genes more activated in
270 *BRL3ox* under drought compared to WT (Supplementary Data 10) and (ii)
271 genes more repressed in *BRL3ox* under drought compared to WT
272 (Supplementary Data 11). GO enrichment analysis of this genotype-drought
273 interaction revealed (i) secondary metabolism, response to stress and response

274 to water deprivation in the first group and (ii) brassinosteroid mediated signaling
275 pathway in the second group (Fig. 5d). Importantly, the expression levels of
276 dehydration response genes kept repressed in *quad* mutant plants during
277 drought (Supplementary Fig. 7 and Supplementary Data 12-15). The
278 expression levels of two key BR biosynthesis genes, *CPD* and *DWF4* were
279 analyzed by RT qPCR. Consistently, within the drought time course,
280 transcription levels of *CPD* and *DWF4* were increased in *quad* and reduced in
281 *BRL3ox* compared to WT plants. Quantification of the bioactive BR hormone
282 Castasterone (CS) showed similar trends and BL hormone was only detected in
283 *quad*, suggesting that BL is accumulated in *quad* more than in WT and *BRL3ox*
284 plants (Supplementary Fig. 9).
285 Analysis of transcription factors revealed 29 of them with differential responses
286 to drought between *BRL3ox* and WT roots. Interestingly, the drought-responsive
287 transcription factor *RD26* showed an enhanced response in *BRL3ox* roots
288 during stress, whereas several vascular-specific transcription factors remained
289 repressed under drought (Supplementary Fig. 10). Given that the BRL3
290 receptor is natively expressed at the phloem-pole pericycle and enriched in
291 vascular tissues when overexpressed [33], we analyzed the spatial distribution of
292 the derregulated genes within the root tissues in our RNAseq dataset [49]. The
293 deregulated genes were preferentially enriched in specific vascular tissues such
294 as the pericycle and phloem pole pericycle but also in lateral root primordia
295 (which initiates from pericycle) and root hair cells, (Fig. 6a, see Methods).
296 Interaction-affected genes concentrated in pericycle and phloem but also in
297 columella and cortex (Fig. 6b). Among the phloem-enriched genes, we found
298 two trehalose phosphatases (*TPPs*) and one galactinol synthases (*GolS2*) that

299 show increased expression in *BRL3ox* roots at basal conditions and in response
300 to drought (Fig. 6d). These enzymes drive the synthesis of the osmoprotectant
301 metabolites — trehalose, myo-inositol and raffinose — we found to be
302 accumulated in *BRL3ox* roots. Together, these results support the importance
303 of increasing BRL3 signaling in the phloem for sustaining drought resistance.
304 Furthermore, a statistical analysis revealed a significant link between the whole
305 transcriptomic and metabolomic signatures, both in basal conditions and under
306 drought (p=0.017 and p=0.001 respectively; see Methods). This indicates that
307 the metabolic signature of *BRL3ox* plants is transcriptionally controlled. We
308 used the metabolic and transcriptomic signatures to identify deregulated
309 metabolic pathways using Paintomics [50]. This analysis revealed a constitutive
310 control of sucrose metabolism by the vascular BRL3 pathway that was
311 enhanced during drought stress in *BRL3ox* plants. We also found that BRL3
312 controls galactose metabolism under periods of drought, including the raffinose
313 family of oligosaccharides (RFOs) synthesis pathway (Supplementary Fig. 11,
314 Supplementary Data 16 and 17). Collectively, these results support that the
315 BRL3 receptor promotes drought tolerance, mainly by controlling sugar
316 metabolism.
317

318 **DISCUSSION**

319 Our study addresses the importance of the BRL3 receptor in preventing growth
320 arrest during severe periods of drought. This is accomplished through the
321 transcriptional control of metabolic pathways that produce osmoprotectant
322 metabolites that are accumulated in the roots. While spatial BR signaling has
323 been shown to contribute to stem cell replenishment in response to genotoxic

324 stress [31,34], here we uncover a role for vascular-enriched BRL3 receptors in
325 promoting growth during drought. Altogether, our results highlight the
326 importance of the spatial regulation of BRL3 signaling in plant stress responses
327 and open a window for studying drought tolerance in plants at a cell-specific
328 resolution.

329 The exogenous application of BR compounds has been used widely in
330 agriculture to extend growth under different abiotic stresses [22,51], yet how these
331 molecules precisely activate growth in challenging conditions remains largely
332 unknown. The analysis of BR signaling and BR synthesis mutant plants
333 subjected to stress failed to provide a linear picture of the involvement of BR in
334 drought stress adaptation. For instance, although overexpression of the
335 canonical BRI1 pathway and the BR biosynthesis gene DWF4 can both confer
336 abiotic stress resistance [24,38], *BRI1* loss-of-function mutants also showed
337 drought stress resistance [2526]. However, increased levels of BR-regulated
338 transcription factors trigger antagonistic effects in drought stress responses [26,52],
339 thus depicting a complex scenario for the role of BRs in abiotic stress. Given the
340 spatiotemporal regulation of the BR signaling components [39] and the complexity
341 of drought traits [7], it is plausible to hypothesize that drought traits are under the
342 control of cell type-specific BR signaling.

343 Our study unveils that the BR family of receptors, in addition to promoting
344 growth, guides phenotypic adaptation responses to a myriad of drought stress
345 traits. The drought resistance phenotypes of BR loss-of-function mutants (Fig.
346 3a) are likely caused by a reduced exposure of these plants to the effect of
347 drought. This phenomenon, known as drought avoidance, is linked to growth
348 arrest and stress insensitivity that maintains transpiration, leaf water status and

349 photosynthesis along the drought (Fig. 3 and Supplementary Fig. 4). The
350 reduced levels of ABA and canonical stress-related metabolites, together with
351 the downregulation of stress genes, further support the insensitivity of *quad*
352 plants to stress (Supplementary Figs. 7 and 8).
353 In contrast, the phenotypes observed in *BRL3ox* plants indicate an active
354 drought tolerance mechanism driven by the BRL3 receptor. First, *BRL3ox* roots
355 showed induced water stress-induced PCD in the root tip compared to WT (Fig.
356 1c,d), which has been proposed to modify the root system architecture and
357 thereby enhance drought tolerance [49]. Second, the enhanced hydrotropic
358 response of *BRL3ox* roots (Fig. 2a-c) could function during water-limited
359 conditions by modifying root architecture for increased acquisition of water,
360 favoring plant growth and survival under drought conditions as previously
361 described [53]. Third, at same RWC in leaves, the rate of photosynthesis and
362 transpiration were more stable in *BRL3ox* than in WT plants during drought (Fig.
363 3d,e and Supplementary Fig. 4). Altogether, these findings indicate that BRL3
364 actively promotes drought tolerance without penalizing plant growth.
365 We found the expression of the drought-response transcription factor *RD26* to
366 be enhanced in *BRL3ox* roots when subjected to drought (Supplementary Fig.
367 10). *RD26* has been shown to antagonize with the BR canonical transcription
368 factor BES1 [26], thereby suggesting that BRL3 activates alternative pathways.
369 These alternative pathways may be derived from a spatial specialization of BR
370 functions within the root. Indeed, we found enriched transcriptional responses
371 within the vascular tissues of *BRL3ox* roots, especially within phloem-related
372 cell types (Fig. 6a,b). The localization of the native BRL3 protein in phloem cells
373 [33] and the metabolic signature found in *BRL3ox* supports its implication in

374 phloem loading during drought. Moreover, metabolic enzymes implicated in
375 trehalose and RFO metabolism were enriched in vascular tissues and either
376 upregulated in *BRL3ox* roots in basal conditions or strongly responding to
377 drought (Fig. 6c,d). Thus, BRL3 function not only loads/unloads the phloem, but
378 also directly controls metabolic pathways. This is the case for the trehalose
379 phosphate phosphatase family (*TPPs*) [54,55] and galactinol synthase 2 (*GolS2*)
380 [56], which are both described to impact drought responses and are involved in
381 trehalose and RFO synthesis respectively. In addition to controlling enzymes at
382 the vascular level, our analyses also uncover a role for BRL3 in mediating non-
383 vascular enzymes important for metabolism and drought responses. These
384 enzymes include hexokinases such as *HXK3* or *HKL1*, the sucrose synthases
385 *SUS3* and *SPS2F*, and proline dehydrogenase genes such as the early
386 response to dehydration 5 (*ERD5)* which is involved in stress tolerance [57]. In
387 light of our findings and given that *Bes1-D* gain-of-function mutants exhibit
388 drought hypersensitivity [26], we propose that vascular BRL3 receptors may act
389 independently of the canonical growth-promoting BRI1 pathway.
390 Our data further suggest that *BRL3ox* plants accumulate sugars in the sink
391 tissues to enable plant roots to grow and escape drought by searching for water
392 within the soil. In support of these findings, we also observed reduced levels of
393 photosynthesis in well-watered leaves of *BRL3ox* plants (Fig. 3e). These
394 results, together with the higher levels of sucrose in roots compared with in
395 shoots (Fig. 4a) and higher levels of glucose and fructose in the shoots suggest
396 that the BRL3 pathway promotes sugar mobilization from the leaves (source) to
397 the roots (sink). In fact, previous work reported that BRs promote the flow of

398 assimilates in crops from source to sink via the vasculature [58] and via sucrose
399 phloem unloading [59].
400 In control conditions, *BRL3ox* plants exhibited a metabolic signature enriched in
401 proline and sugars. Proline and sugar accumulation classically correlates with
402 drought stress tolerance, osmolytes, ROS scavengers, and chaperone functions
403 [5,45-47,60,61], suggesting that the BRL3 receptor promotes priming [48,62]. In addition,
404 *BRL3ox* plants also accumulated succinate, fumarate and malate. Importantly,
405 all these metabolites were decreased in *quad* mutant plants. Altogether, these
406 data uncover a role for BRL3 signaling in the promotion of the tricarboxylic acid
407 (TCA) cycle, sugar and amino acid metabolism.
408 In drought stress conditions, *BRL3ox* shoots displayed increased levels of the
409 amino acids proline, GABA and tyrosine. In contrast, trehalose, sucrose, *myo*-
410 inositol, raffinose, and proline were the most abundant metabolites in the
411 *BRL3ox* roots along the stress time course. Importantly, all these metabolites
412 have previously been linked to drought resistance [45,46,60]. In addition, the levels
413 of the RFO metabolites raffinose and *myo*-inositol, which are involved in
414 membrane protection and radical scavenging [63], were higher in the roots of
415 *BRL3ox* plants under drought, yet reduced in the roots of *quad* plants.
416 Our data indicate that the roots of *BRL3ox* plants are loaded with
417 osmoprotectant metabolites and are thus better prepared to alleviate drought
418 stress via a phenomenon previously referred to as priming [48,62]. Further
419 supporting our hypothesis, the BRL3 signalosome is enriched in abiotic stress
420 proteins [33]. Altogether these data suggest that drought stress responses are
421 correlated with BRL3 receptor levels in the root vasculature, especially within
422 the phloem, and that this is key for the greater survival rates of *BRL3ox* plants.

423 Future cell type-specific engineering of signaling cascades stands out as a
424 promising strategy to circumvent growth arrest caused by drought stress.
425
426 **METHODS**
427 **Plant materials**
428 Seeds were sterilized with 35% NaClO for 5 min and washed five times for 5min
429 with sterile dH_2O. Sterile seeds were vernalized 48 h at 4ºC and grown in half-
430 strength agar Murashige and Skoog (MS1/2) media with vitamins and without
431 sucrose. Plates were grown vertically in long day (LD) conditions (16 h of light /
432 8 h of dark; 22°C, 60% relative humidity). Genotypes used in this study:
433 Columbia-0 WT (Col-0 WT), *brl1-1brl3-1* (*brl1brl3*), *bak1-3* (*bak1*), *bri1-301*
434 (*bri1*), *bri1-301brl1-1brl3-1* (*bri1brl1brl3*), *bri1-301bak1-3brl1-1brl3-1 (quad)* and
435 *35S:BRL3-GFP (BRL3ox)* [33]. DNA rapid extraction protocol [64] was used for all
436 the plant genotyping experiments. Supplementary Table 2 describes the
437 primers used for genotyping of the BR mutant plants.
438
439 **Brassinolide and sorbitol sensitivity assays in roots**
440 For hormone treatments, seeds were continuously grown in concentration
441 series of brassinolide (BL,Wako, Japan). For sorbitol assays, three-day-old
442 seedlings were transferred to either control or 270 mM sorbitol media for four
443 additional days. The root length of seven-day-old seedlings was measured
444 using Image J (http://rsb.info.nih.gov/ij/) and compared with automatically
445 acquired data from the MyROOT [65] software (Supplementary Fig. 13). Four-day-
446 old roots grown in control conditions or in 24 h of sorbitol were stained with
447 propidium iodide (10 ug/ml, PI, Sigma). PI stains the cell wall (control) and DNA

448 in the nuclei upon cell death (sorbitol). Images were acquired with a confocal
449 microscope (FV1000 Olympus). Cell death damage in primary roots was
450 measured in a window of 500 µm from QC in the middle root longitudinal
451 section (Image J). As an arbitrary setting to measure the stained area, a color
452 threshold ranging from 160 to 255 in brightness was selected.
453
454 **Root hydrotropism**
455 Seedlings were germinated in MS1/2 without sucrose for six days. Then, the
456 lower part of the agar was removed from the plates and MS1/2 with 270 mM
457 sorbitol was added to simulate a situation of reduced water availability. The
458 media was placed in 45-degree angle to scape gravitropism effect. When
459 indicated, 1 µM of brassinazole [44] was added to sorbitol media. Root curvature
460 angles were measured and analyzed using the Image J software
461 (http://rsb.info.nih.gov/ij/).
462
463 **Drought stress for scoring plant survival**
464 One-week-old seedlings grown in MS1/2 agar plates were transferred
465 individually to pots containing 30±1 g of substrate (plus 1:8 v/v vermiculite and
466 1:8 v/v perlite). For each biological replicate, 40 plants of each genotype were
467 grown in LD conditions for three weeks. Three-week-old plants were subjected
468 to severe drought stress by withholding water for 12 days followed by re-
469 watering. After the seven-day recovery period, the surviving plants were
470 photographed and manually counted (two-sided chi-squared test, p-value
471 <0.01).
472

473 **Metabolite profiling analyses**

474 One-week-old seedlings were placed in individual pots with 30 g of autoclaved
475 soil and grown under LD photoperiodic conditions. After three weeks growing,
476 half of the plants were subjected to severe drought (withholding water) for six
477 days and the other half were watered normally (well-watered control conditions).
478 A total of five biological replicates were collected every 24 h during the time
479 course (from day 0 to day 6) both in drought and watered conditions and for
480 each genotype (WT, *quad* and *BRL3ox*). Four independent plants were bulked
481 in each biological replicate. Roots were manually separated from shoots. Four
482 entire shoots were grinded using the Frosty Cryogenic grinder system
483 (Labman). Four entire root samples were grinded in the Tissue Lyser Mixer-Mill
484 (Qiagen). Roots were aliquoted into 20 mg samples and shoot into 50 mg
485 samples (the exact weight was annotated for data normalization). Primary
486 metabolite extraction was carried as follows [66]. One Zirconia and 500 µl of 100%
487 Methanol premixed with Ribitol (20:1) were added and samples were
488 subsequently homogenized in the Tissue Lyser (Qiagen) 3 min at 25 Hz.
489 Samples were centrifuged 10 min at 14000 rpm (10 ºC) and resulting
490 supernatant was transferred into fresh tubes. Addition of 200 µl of CHCl3 and
491 vortex ensuring one single phase followed by the addition of 600 µl of H20 and
492 vortex 15 sec. Samples were centrifuged 10 min at 14000 rpm (10 ºC). 100 µl
493 from the upper phase (polar phase) were transferred into fresh eppendorf tubes
494 (1.5 ml) and dried in the speed vacuum for at least 3 h without heating. 40 µl of
495 derivatization agent (methoxyaminhydrochloride in pyridine) were added to
496 each sample (20 mg/ml). Samples were shaken during 3 h at 900 rpm at 37 ºC.
497 Drops on the cover were shortly spun down. One sample vial with 1 mL MSTFA

498 + 20 µl FAME mix was prepared. Addition of 7 0µl MSTFA + FAMEs in each
499 sample was done followed by shaking 30 min at 37 ºC. Drops on the cover were
500 shortly spun down.
501 Samples were transferred into glass vials specific for injection in GC-TOF-MS.
502 The GC-TOF-MS system comprised of a CTC CombiPAL autosampler, an
503 Agilent 6890N gas chromatograph, and a LECO Pegasus III TOF-MS running in
504 EI+ mode. Metabolites were identified by comparing to database entries of
505 authentic standards [67]. Chromatograms were evaluated using Chroma TOF 1.0
506 (Leco) Pegasus software was used for peak identification and correction of RT.
507 Mass spectra were evaluated using the TagFinder 4.0 software [68] for metabolite
508 annotation and quantification (peak area measurements). The resulting data
509 matrix was normalized using an internal standard, Ribitol, in 100% methanol
510 (20:1), followed by normalization with the fresh weight of each sample.
511 Metabolomics data from control (well-watered) conditions at day 0 were
512 analyzed with a two-tailed t-test, p-value<0.05 (no multiple testing correction).
513 Data from the time course was analyzed with R software using the maSigPro
514 package [69]. Briefly, the profile of each metabolite under each condition was
515 fitted to a polynomial model of maximum degree 3. The curves of each
516 genotype were statistically compared taking into account the fitting value and
517 correcting the p-value (Benjamini-Hochberg method). Significant metabolites (p-
518 value < 0.05) having a differential profile between genotypes were plotted to
519 visualize their behavior under the drought time course. Clustering analysis was
520 performed using the maSigPro package and the *hclust* R core function.
521
522 **Transcriptomic profiling analysis**

523 For microarray analysis, a drought stress time course was carried out in WT
524 and *quad* mutant three-week-old plants. Entire plants grown under drought
525 stress and control conditions were collected every 48 h during the time course
526 (Day 0, Day 2 and Day 4). Two biological replicates composed of five
527 independent rosettes were collected. RNA was extracted with the Plant Easy
528 Mini Kit (Qiagen) and quality checked using the Bioanalyser. A Genome-Wide
529 Microarray platform (Dual color, Agilent) was performed by swapping the color
530 hybridization of each biological replicate (Cy3 and Cy5). Statistical analysis was
531 performed with the package "limma" [70], and the "mle2/"normexp" background
532 correction method was used. Different microarrays were quantile-normalized
533 and a Bayes test used to identify differentially expressed probes. The results
534 were filtered for adjusted p-value<0.05 (after Benjamini-Hochberg correction)
535 and Log2 FC >|1.5|. For RNAseq analysis, three-week-old roots were detached
536 from mature plants grown in soil under control conditions and five days of
537 drought. RNA was extracted as described above. Stranded cDNA libraries were
538 prepared with TruSeq Stranded mRNA kit (Illumina). Single-end sequencing,
539 with 50-bp reads, was performed in an Illumina HiSeq500 sequencer, at a
540 minimum sequencing depth of 21 M. Reads were trimmed 5 bp at their 3' end,
541 quality filtered and then mapped against the TAIR10 genome with "HISAT2".
542 Mapped reads were quantified at the gene level with "HtSeq". For differential
543 expression, samples were TMM normalized and statistical values calculated
544 with the "EdgeR" package in R. Results were filtered for adjusted p-value (FDR)
545 <0.05 and FC >|2| in the pairwise comparisons. For the evaluation of differential
546 drought response between WT and *BRL3ox* roots, a lineal model accounting for
547 the interaction genotype and drought was constructed with "EdgeR" package.

548 The interaction term was evaluated. A gene was considered to be affected by
549 the interaction if p-value (uncorrected) < 0.0025. Heatmaps were performed in
550 R with the heatmap.2 function implemented in the "gplots" package.
551 For the Rt qPCR, cDNA was obtained from RNA samples by using the
552 Transcriptor First Strand cDNA Synthesis Kit (Roche) with oligo dT primers.
553 qPCR amplifications were performed from 10ng of cDNA using LightCycler 480
554 SYBR Green I master mix (Roche) in 96-well plates according the manufacturer
555 recommendations. The Real Time PCR was performed on a LightCycler 480
556 System (Roche). Ubiquitin (AT5G56150) was used as housekeeping gene for
557 relativizing expression. Primers used are described in Supplementary Table 3.
558
559 **Statistical methods, and omics data integration.**
560 For root tissue enrichment analysis, deregulated genes were queried against
561 available lists of tissue-enriched genes [49]. For each tissue, a 2x2 contingency
562 table was constructed, counting the number of deregulated genes in the tissue
563 that were enriched and non-enriched and also the number of non-deregulated
564 genes (for either FDR>0.05 or logFC >/< in the RNAseq gene universe) that
565 were enriched and non-enriched. Statistical values of the enrichment were
566 obtained using a one-sided Fisher's test. To statistically evaluate the influence
567 of transcriptomic changes on the metabolic signature, both deregulated
568 enzymes and metabolites were queried in an annotation file of the metabolic
569 reactions of *Arabidopsis thaliana*, which included merged data from the KEGG
570 (http://www.genome.jp/kegg/) and BRENDA (www.brenda-enzymes.org)
571 databases. Then, the same approach of constructing a 2x2 contingency table
572 was taken. Significant and non-significant metabolites annotated in the

573 database were matched with differentially and non-differentially expressed
574 genes annotated in the database. The statistical value of the association
575 between regulated metabolites and genes was obtained through a two-sided
576 Fisher's exact test. Genes and metabolites were mapped onto the KEGG
577 pathways using the PaintOmics3 (http://bioinfo.cipf.es/paintomics/) according
578 the developer´s instructions [50].
579
580 **Physiological parameters and chlorophyll fluorescence**
581 One-week-old seedlings were placed in individual pots and watered with the
582 same volume of a modified Hoagland solution (one-fifth strength). Pots were
583 weighed daily during the experiment. Well-watered control plants were grown in
584 100% field capacity (0% of water loss). The time course drought stress assay
585 was started by withholding the nutrient solution until reaching 25, 50, 60 and
586 70% water loss. Photosynthesis (*A*) and transpiration (*E*) were measured in
587 control and drought plants at those time points. Four plants of each genotype
588 were harvested at 0, 50 and 70% water loss for biomass, water content and
589 hormone analyses. Drought experiments were repeated three times and at least
590 four plants per genotype and treatment were used in each experiment. RWC
591 was calculated according to the formula: RWC (%) = [(FW-DW) / (TW-DW)] x
592 100.
593
594 **Plant hormones quantification**
595 Plant hormones cytokinins (*trans*-zeatin), gibberellins (GA1, GA4 and GA3),
596 indole-3-acetic acid (IAA), abscisic acid (ABA), salicylic acid (SA), jasmonic acid
597 (JA), and the ethylene precursor 1-aminocyclopropane-1-carboxylic acid (ACC)

598 were analyzed as follows. 10 µl of extracted sample were injected in a UHPLC–
599 MS system consisting of an Accela Series U-HPLC (ThermoFisher Scientific,
600 Waltham, MA, USA) coupled to an Exactive mass spectrometer (ThermoFisher
601 Scientific, Waltham, MA, USA) using a heated electrospray ionization (HESI)
602 interface. Mass spectra were obtained using the Xcalibur software version 2.2
603 (ThermoFisher Scientific, Waltham, MA, USA). For quantification, calibration
604 curves were constructed for each analyzed hormone (1, 10, 50, and 100 µg l−1)
605 and corrected for 10 µg l−1 deuterated internal standards. Recovery
606 percentages ranged between 92 and 95%.
607 For endogenous BR analysis plant materials (4 g fresh weight) were lyophilized
608 and grinded. BL and CS were extracted with methanol and purified by solvent
609 partitions by using a silica gel column and ODS-HPLC as follows. The
610 endogenous levels of BL and CS were quantified by LC-MS/MS using their
611 deuterated internal standards (2ng).
612 LC-MS/MS analysis was performed with a triple quadrupole/linear ion trap
613 instrument (QTRAP5500; AB Sciex, USA) with an electrospray source. Ion
614 source was maintained at 300 ≠C. Ionspray voltage was set at 4500 V in
615 positive ion mode. MRM analysis were performed at the transitions of m/z 487
616 to 433 (Collision Energy, CE 30 V) and 487 to 451 (CE 21 V) for 2 H 6 -BL, m/z
617 481 to 427 (CE 30 V) and 481 to 445 (CE 30 V) for BL, m/z 471 to 435 (CE 23
618 V) and 471 to 453 (CE 25 V) for 2 H 6 -CS and m/z 465 to 429 (CE 23 V) and
619 465 to 447 (CE 25 V) for CS. Enhanced product ion scan was carried out at CE
620 21 V. HPLC separation was performed using a UHPLC (Nexera X2; Shimadzu,
621 Japan) equipped with an ODS column (Kinetex C18, f2.1 ‘ 150 mm, 1.7 µm;
622 Phenomenex, USA). The column oven temperature was maintained at 30ºC.

623 The mobile phase consisted of acetonitrile (solvent A) and water (solvent B),
624 both of which contained 0.1% (v/v) acetic acid. HPLC separation was conducted
625 with the following gradient at flow rate of 0.2 mL·min-1: 0 to 12 min, 20% A to
626 80% A; 12 to 13 min, 80% A to 100% A; 13 to 16 min, 100% A.
627

628 **DATA AVAILABILITY**

629 RNAseq and microarray data that support the findings of this study have been
630 deposited in Gene Expression Omnibus (GEO) with the GSE119382 and
631 GSGE119383 accession codes.
632 [https://www.ncbi.nlm.nih.gov/geo/query/acc.cgi?acc=GSE119382"]
633 [https://www.ncbi.nlm.nih.gov/geo/query/acc.cgi?acc=GSE119383]
634
635

636 **COMPETING INTERESTS**

637 The authors declare no competing interests.
638

639 **ACKNOWLEDGEMENTS**

640 We thank Riccardo Aiese Cigliano (Sequentia Biotech) for help with microarray
641 analysis, Tony Ferrar for critical manuscript revision and language editing
642 (http://www.theeditorsite.com)and Olga Moreno Pradas for graphic design
643 support. We acknowledge financial support from the Spanish Ministry of
644 Economy and Competitiveness, through the "Severo Ochoa Programme for
645 Centres of Excellence in R&D" 2016-2019 (SEV-2015-0533)", the CERCA
646 Programme from the Generalitat de Catalunya, and the Agencia de Gestió
647 d'Ajuts Universitaris i de Recerca (2014 SGR 1406). N.F. was funded by

Fundación Renta Corporación, by EMBO short-term postdoctoral fellowship (ASTF 422-2015) and by BIO2013-43873; F.L.E was funded by BIO2013-43873 and BIO2016-78150-P; and D.B. was funded by BIO2013-43873 and ERC-2015-CoG-GA 683163. CMA, AA and FPA acknowledge financial support from the Spanish MINECO-FEDER (project AGL2014-59728-R) and from the European Union's Seventh Framework Programme for research technological development and demonstration under grant agreement no. 289365 (project ROOTOPOWER). S.O. was supported by Ministry of Science and Innovation and University of Malaga (Spain) through the grant Ramón y Cajal program (Sonia Osorio, RYC-09170). M.B was funded by BES-2012-053274 and J.L.R laboratory is supported by grant BFU2014-58289-P from the Spanish Ministry of Economy and Competitiveness. A.I.C.-D. – A.C. collaboration was funded by the European Regional Development Funds and Marie Curie IRSES Project DEANN (PIRSES-GA-2013-612583). A.I.C.-D. is a recipient of BIO2013-43873 and BIO2016-78150-P grants from the Spanish Ministry of Economy and Competitiveness. A.I.C.-D. is recipient of an ERC Consolidator Grant ; this project has received funding from the European Research Council (ERC) under the European Union's Horizon 2020 research and innovation program (grant agreement No 683163).

AUTHOR CONTRIBUTIONS

A.I.C.-D conceived, designed and supervised the study. N.F., F.L.E, D.B., C.M.A. and F.P.A. performed the genetics and stress phenomic experiments and data analyses. N.F., F.L.E., M.B., J.L.R. and A.C.D. designed the genome-wide experiments. N.F., F.L.E., A.C. and A.C.D. performed the genome-wide

experiments and data analysis. N.F., F.L.E., T.T., S.O., and A.R.F. carried out the metabolite and data analysis. A.A. performed the hormone profiling experiments. T.N. and T.Y. carried the CS and BL quantification assays. N.F., F.L.E and A.C.D. wrote the manuscript. All authors discussed the results and the manuscript.

698 **REFERENCES**

699 1 Boyer, J. S. Plant productivity and environment. *Science* **218**, 443-448,
700 doi:10.1126/science.218.4571.443 (1982).

701 2 Todaka, D., Shinozaki, K. & Yamaguchi-Shinozaki, K. Recent advances
702 in the dissection of drought-stress regulatory networks and strategies for
703 development of drought-tolerant transgenic rice plants. *Front Plant Sci* **6**,
704 84, doi:10.3389/fpls.2015.00084 (2015).

705 3 Yoshida, T., Mogami, J. & Yamaguchi-Shinozaki, K. ABA-dependent and
706 ABA-independent signaling in response to osmotic stress in plants. *Curr*
707 *Opin Plant Biol* **21**, 133-139, doi:10.1016/j.pbi.2014.07.009 (2014).

708 4 Graether, S. P. & Boddington, K. F. Disorder and function: a review of
709 the dehydrin protein family. *Front Plant Sci* **5**, 576,
710 doi:10.3389/fpls.2014.00576 (2014).

711 5 Seki, M., Umezawa, T., Urano, K. & Shinozaki, K. Regulatory metabolic
712 networks in drought stress responses. *Curr Opin Plant Biol* **10**, 296-302,
713 doi:10.1016/j.pbi.2007.04.014 (2007).

714 6 Shao, H. B., Chu, L. Y., Jaleel, C. A. & Zhao, C. X. Water-deficit stress-
715 induced anatomical changes in higher plants. *C R Biol* **331**, 215-225,
716 doi:10.1016/j.crvi.2008.01.002 (2008).

717 7 Tardieu, F. Any trait or trait-related allele can confer drought tolerance:
718 just design the right drought scenario. *J Exp Bot* **63**, 25-31,
719 doi:10.1093/jxb/err269 (2012).

720 8 Marshall, A. *et al.* Tackling drought stress: receptor-like kinases present
721 new approaches. *Plant Cell* **24**, 2262-2278, doi:10.1105/tpc.112.096677
722 (2012).

723 9 Smakowska-Luzan, E. *et al.* An extracellular network of Arabidopsis
724 leucine-rich repeat receptor kinases. *Nature* **553**, 342-346,
725 doi:10.1038/nature25184 (2018).
726 10 Li, J. & Chory, J. A putative leucine-rich repeat receptor kinase involved
727 in brassinosteroid signal transduction. *Cell* **90**, 929-938 (1997).
728 11 Wang, Z. Y., Seto, H., Fujioka, S., Yoshida, S. & Chory, J. BRI1 is a
729 critical component of a plasma-membrane receptor for plant steroids.
730 *Nature* **410**, 380-383, doi:10.1038/35066597 (2001).
731 12 Kinoshita, T. *et al.* Binding of brassinosteroids to the extracellular domain
732 of plant receptor kinase BRI1. *Nature* **433**, 167-171,
733 doi:10.1038/nature03227 (2005).
734 13 Hothorn, M. *et al.* Structural basis of steroid hormone perception by the
735 receptor kinase BRI1. *Nature* **474**, 467-471, doi:10.1038/nature10153
736 (2011).
737 14 She, J. *et al.* Structural insight into brassinosteroid perception by BRI1.
738 *Nature* **474**, 472-476, doi:10.1038/nature10178 (2011).
739 15 Karlova, R. *et al.* The Arabidopsis SOMATIC EMBRYOGENESIS
740 RECEPTOR-LIKE KINASE1 protein complex includes
741 BRASSINOSTEROID-INSENSITIVE1. *Plant Cell* **18**, 626-638,
742 doi:10.1105/tpc.105.039412 (2006).
743 16 Li, J. *et al.* BAK1, an Arabidopsis LRR receptor-like protein kinase,
744 interacts with BRI1 and modulates brassinosteroid signaling. *Cell* **110**,
745 213-222 (2002).
746 17 Nam, K. H. & Li, J. BRI1/BAK1, a receptor kinase pair mediating
747 brassinosteroid signaling. *Cell* **110**, 203-212 (2002).

748 18 Gou, X. *et al.* Genetic evidence for an indispensable role of somatic
749 embryogenesis receptor kinases in brassinosteroid signaling. *PLoS*
750 *Genet* **8**, e1002452, doi:10.1371/journal.pgen.1002452 (2012).
751 19 Yin, Y. *et al.* BES1 accumulates in the nucleus in response to
752 brassinosteroids to regulate gene expression and promote stem
753 elongation. *Cell* **109**, 181-191 (2002).
754 20 Wang, Z. Y. *et al.* Nuclear-localized BZR1 mediates brassinosteroid-
755 induced growth and feedback suppression of brassinosteroid
756 biosynthesis. *Dev Cell* **2**, 505-513 (2002).
757 21 He, J. X., Gendron, J. M., Yang, Y., Li, J. & Wang, Z. Y. The GSK3-like
758 kinase BIN2 phosphorylates and destabilizes BZR1, a positive regulator
759 of the brassinosteroid signaling pathway in Arabidopsis. *Proc Natl Acad*
760 *Sci U S A* **99**, 10185-10190, doi:10.1073/pnas.152342599 (2002).
761 22 Kagale, S., Divi, U. K., Krochko, J. E., Keller, W. A. & Krishna, P.
762 Brassinosteroid confers tolerance in Arabidopsis thaliana and Brassica
763 napus to a range of abiotic stresses. *Planta* **225**, 353-364,
764 doi:10.1007/s00425-006-0361-6 (2007).
765 23 Krishna, P. Brassinosteroid-Mediated Stress Responses. *J Plant Growth*
766 *Regul* **22**, 289-297, doi:10.1007/s00344-003-0058-z (2003).
767 24 Sahni, S. *et al.* Overexpression of the brassinosteroid biosynthetic gene
768 DWF4 in Brassica napus simultaneously increases seed yield and stress
769 tolerance. *Sci Rep* **6**, 28298, doi:10.1038/srep28298 (2016).
770 25 Feng, Y., Yin, Y. & Fei, S. Down-regulation of BdBRI1, a putative
771 brassinosteroid receptor gene produces a dwarf phenotype with

772 enhanced drought tolerance in Brachypodium distachyon. *Plant Sci* **234**,
773 163-173, doi:10.1016/j.plantsci.2015.02.015 (2015).
774 26 Ye, H. *et al.* RD26 mediates crosstalk between drought and
775 brassinosteroid signalling pathways. *Nat Commun* **8**, 14573, doi:10.1038/
776 ncomms14573 (2017).
777 27 Zhang, S., Cai, Z. & Wang, X. The primary signaling outputs of
778 brassinosteroids are regulated by abscisic acid signaling. *Proc Natl Acad*
779 *Sci U S A* **106**, 4543-4548, doi:10.1073/pnas.0900349106 (2009).
780 28 Gui, J. *et al.* OsREM4.1 Interacts with OsSERK1 to Coordinate the
781 Interlinking between Abscisic Acid and Brassinosteroid Signaling in Rice.
782 *Dev Cell* **38**, 201-213, doi:10.1016/j.devcel.2016.06.011 (2016).
783 29 Huang, D., Wu, W., Abrams, S. R. & Cutler, A. J. The relationship of
784 drought-related gene expression in Arabidopsis thaliana to hormonal and
785 environmental factors. *J Exp Bot* **59**, 2991-3007, doi:10.1093/jxb/ern155
786 (2008).
787 30 Chung, Y., Kwon, S. I. & Choe, S. Antagonistic regulation of Arabidopsis
788 growth by brassinosteroids and abiotic stresses. *Mol Cells* **37**, 795-803,
789 doi:10.14348/molcells.2014.0127 (2014).
790 31 Vilarrasa-Blasi, J. *et al.* Regulation of plant stem cell quiescence by a
791 brassinosteroid signaling module. *Dev Cell* **30**, 36-47,
792 doi:10.1016/j.devcel.2014.05.020 (2014).
793 32 Fàbregas, N. & Caño-Delgado, A. I. Turning on the microscope turret: a
794 new view for the study of brassinosteroid signaling in plant development.
795 *Physiol Plant* **151**, 172-183, doi:10.1111/ppl.12130 (2014).

796 33 Fàbregas, N. *et al.* The brassinosteroid insensitive1-like3 signalosome
797 complex regulates Arabidopsis root development. *Plant Cell* **25**, 3377-
798 3388, doi:10.1105/tpc.113.114462 (2013).
799 34 Lozano-Elena, F., Planas-Riverola, A., Vilarrasa-Blasi, J., Schwab, R. &
800 Cano-Delgado, A. I. Paracrine brassinosteroid signaling at the stem cell
801 niche controls cellular regeneration. *J Cell Sci* **131**, jcs204065
802 doi:10.1242/jcs.204065 (2018).
803 35 Friedrichsen, D. M., Joazeiro, C. A., Li, J., Hunter, T. & Chory, J.
804 Brassinosteroid-insensitive-1 is a ubiquitously expressed leucine-rich
805 repeat receptor serine/threonine kinase. *Plant Physiol* **123**, 1247-1256
806 (2000).
807 36 Caño-Delgado, A. *et al.* BRL1 and BRL3 are novel brassinosteroid
808 receptors that function in vascular differentiation in Arabidopsis.
809 *Development* **131**, 5341-5351, doi:10.1242/dev.01403 (2004).
810 37 Belkhadir, Y. & Jaillais, Y. The molecular circuitry of brassinosteroid
811 signaling. *New Phytol* **206**, 522-540, doi:10.1111/nph.13269 (2015).
812 38 Eremina, M. *et al.* Brassinosteroids participate in the control of basal and
813 acquired freezing tolerance of plants. *Proc Natl Acad Sci U S A* **113**,
814 E5982-E5991, doi:10.1073/pnas.1611477113 (2016).
815 39 Vragovic, K. *et al.* Translatome analyses capture of opposing tissue-
816 specific brassinosteroid signals orchestrating root meristem
817 differentiation. *Proc Natl Acad Sci U S A* **112**, 923-928,
818 doi:10.1073/pnas.1417947112 (2015).

819 40 González-García, M. P. *et al.* Brassinosteroids control meristem size by
820 promoting cell cycle progression in Arabidopsis roots. *Development* **138**,
821 849-859, doi:10.1242/dev.057331 (2011).
822 41 Hacham, Y. *et al.* Brassinosteroid perception in the epidermis controls
823 root meristem size. *Development* **138**, 839-848, doi:10.1242/dev.061804
824 (2011).
825 42 Duan, Y. *et al.* An endoplasmic reticulum response pathway mediates
826 programmed cell death of root tip induced by water stress in Arabidopsis.
827 *New Phytol* **186**, 681-695, doi:10.1111/j.1469-8137.2010.03207.x (2010).
828 43 Takahashi, N., Goto, N., Okada, K. & Takahashi, H. Hydrotropism in
829 abscisic acid, wavy, and gravitropic mutants of Arabidopsis thaliana.
830 *Planta* **216**, 203-211, doi:10.1007/s00425-002-0840-3 (2002).
831 44 Asami, T. *et al.* Characterization of brassinazole, a triazole-type
832 brassinosteroid biosynthesis inhibitor. *Plant Physiol* **123**, 93-100 (2000).
833 45 Singh, T. N., Aspinall, D. & Paleg, L. G. Proline accumulation and varietal
834 adaptability to drought in barley: a potential metabolic measure of
835 drought resistance. *Nat New Biol* **236**, 188-190 (1972).
836 46 Szabados, L. & Savoure, A. Proline: a multifunctional amino acid. *Trends*
837 *Plant Sci* **15**, 89-97, doi:10.1016/j.tplants.2009.11.009 (2010).
838 47 Durand, M. *et al.* Water Deficit Enhances C Export to the Roots in
839 Arabidopsis thaliana Plants with Contribution of Sucrose Transporters in
840 Both Shoot and Roots. *Plant Physiol* **170**, 1460-1479,
841 doi:10.1104/pp.15.01926 (2016).
842 48 Conrath, U., Pieterse, C. M. & Mauch-Mani, B. Priming in plant-pathogen
843 interactions. *Trends Plant Sci* **7**, 210-216 (2002).

844 49 Brady, S. M. *et al.* A high-resolution root spatiotemporal map reveals
845 dominant expression patterns. *Science* **318**, 801-806,
846 doi:10.1126/science.1146265 (2007).
847 50 García-Alcalde, F., García-López, F., Dopazo, J. & Conesa, A.
848 Paintomics: a web based tool for the joint visualization of transcriptomics
849 and metabolomics data. *Bioinformatics* **27**, 137-139,
850 doi:10.1093/bioinformatics/btq594 (2011).
851 51 Shakirova, F. *et al.* Involvement of dehydrins in 24-epibrassinolide-
852 induced protection of wheat plants against drought stress. *Plant*
853 *Physiology and Biochemistry* **108**, 539-548,
854 doi:10.1016/j.plaphy.2016.07.013 (2016).
855 52 Chen, J. *et al.* Arabidopsis WRKY46, WRKY54, and WRKY70
856 Transcription Factors Are Involved in Brassinosteroid-Regulated Plant
857 Growth and Drought Responses. *The Plant Cell* **29**, 1425 (2017).
858 53 Iwata, S., Miyazawa, Y., Fujii, N. & Takahashi, H. MIZ1-regulated
859 hydrotropism functions in the growth and survival of Arabidopsis thaliana
860 under natural conditions. *Ann Bot* **112**, 103-114, doi:10.1093/aob/mct098
861 (2013).
862 54 Ge, L.-F. *et al.* Overexpression of the trehalose-6-phosphate
863 phosphatase gene OsTPP1 confers stress tolerance in rice and results in
864 the activation of stress responsive genes. *Planta* **228**, 191-201,
865 doi:10.1007/s00425-008-0729-x (2008).
866 55 Nuccio, M. L. *et al.* Expression of trehalose-6-phosphate phosphatase in
867 maize ears improves yield in well-watered and drought conditions.
868 *Nature Biotechnology* **33**, 862, doi:10.1038/nbt.3277 (2015).

869 56 Himuro, Y. *et al.* Arabidopsis galactinol synthase AtGolS2 improves
870 drought tolerance in the monocot model Brachypodium distachyon.
871 *Journal of Plant Physiology* **171**, 1127-1131,
872 doi:10.1016/j.jplph.2014.04.007 (2014).
873 57 Nanjo, T. *et al.* Antisense suppression of proline degradation improves
874 tolerance to freezing and salinity in Arabidopsis thaliana. *FEBS Letters*
875 **461**, 205-210, doi:10.1016/S0014-5793(99)01451-9 (1999).
876 58 Wu, C. Y. *et al.* Brassinosteroids regulate grain filling in rice. *Plant Cell*
877 **20**, 2130-2145, doi:10.1105/tpc.107.055087 (2008).
878 59 Xu, F., Xi, Z.-m., Zhang, H., Zhang, C.-j. & Zhang, Z.-w. Brassinosteroids
879 are involved in controlling sugar unloading in Vitis vinifera 'Cabernet
880 Sauvignon' berries during véraison. *Plant Physiology and Biochemistry*
881 **94**, 197-208, doi:10.1016/j.plaphy.2015.06.005 (2015).
882 60 Krasensky, J. & Jonak, C. Drought, salt, and temperature stress-induced
883 metabolic rearrangements and regulatory networks. *J Exp Bot* **63**, 1593-
884 1608, doi:10.1093/jxb/err460 (2012).
885 61 Urano, K. *et al.* Characterization of the ABA-regulated global responses
886 to dehydration in Arabidopsis by metabolomics. *Plant J* **57**, 1065-1078,
887 doi:10.1111/j.1365-313X.2008.03748.x (2009).
888 62 Ding, Y., Fromm, M. & Avramova, Z. Multiple exposures to drought 'train'
889 transcriptional responses in Arabidopsis. *Nat Commun* **3**, 740,
890 doi:10.1038/ncomms1732 (2012).
891 63 Nishizawa, A., Yabuta, Y. & Shigeoka, S. Galactinol and raffinose
892 constitute a novel function to protect plants from oxidative damage. *Plant*
893 *Physiol* **147**, 1251-1263, doi:10.1104/pp.108.122465 (2008).

894 64 Aljanabi, S. M. & Martinez, I. Universal and rapid salt-extraction of high
895 quality genomic DNA for PCR-based techniques. *Nucleic Acids Res* **25**,
896 4692-4693 (1997).
897 65 Betegón-Putze, I., González, A., Sevillano, X., Blasco-Escámez, D. &
898 Caño-Delgado, A. I. . MyROOT: A novel method and software for the
899 semi-automatic measurement of plant root length. Preprint at *bioRxiv*
900 doi:10.1101/309773 (2018).
901 66 Lisec, J., Schauer, N., Kopka, J., Willmitzer, L. & Fernie, A. R. Gas
902 chromatography mass spectrometry-based metabolite profiling in plants.
903 *Nat Protoc* **1**, 387-396, doi:10.1038/nprot.2006.59 (2006).
904 67 Kopka, J. *et al.* GMD@CSB.DB: the Golm Metabolome Database.
905 *Bioinformatics* **21**, 1635-1638, doi:10.1093/bioinformatics/bti236 (2005).
906 68 Luedemann, A., Strassburg, K., Erban, A. & Kopka, J. TagFinder for the
907 quantitative analysis of gas chromatography--mass spectrometry (GC-
908 MS)-based metabolite profiling experiments. *Bioinformatics* **24**, 732-737,
909 doi:10.1093/bioinformatics/btn023 (2008).
910 69 Conesa, A., Nueda, M. J., Ferrer, A. & Talon, M. maSigPro: a method to
911 identify significantly differential expression profiles in time-course
912 microarray experiments. *Bioinformatics* **22**, 1096-1102,
913 doi:10.1093/bioinformatics/btl056 (2006).
914 70 Ritchie, M. E. *et al.* limma powers differential expression analyses for
915 RNA-sequencing and microarray studies. *Nucleic Acids Res* **43**, e47,
916 doi:10.1093/nar/gkv007 (2015).
917
918

919 **FIGURE LEGENDS**

920 **Figure 1. BR perception mutant roots are less sensitive to osmotic stress.**
921 (**a**) Seven-day-old roots of WT, BR mutants *bak1*, *brl1brl3, brl1brl3bak1*, *bri1,*
922 *bri1brl1brl3*, and *bri1brl1brl3bak1* (*quad*), and BR overexpressor line
923 *35S:BRL3-GFP (BRL3ox)* grown in control (-) or 270 mM sorbitol (+) conditions.
924 Scale bar: 0.5 cm. (**b**) Boxplots depict the distribution of seven-day-old root
925 lengths in control (dark green) or sorbitol (light green) conditions. Red line
926 depicts relative root growth inhibition upon stress (ratio sorbitol/control +/-
927 s.e.m.). Data from five independent biological replicates (n>150). Different
928 letters represent significant differences (p-value<0.05) in an ANOVA plus
929 Tukey's HSD test. (**c**) Four-day-old roots stained with propidium iodide (PI, red)
930 after 24 h in control (top) or sorbitol (bottom) media. Green channel (GFP)
931 shows the BRL3 membrane protein receptor under the 35SCaMV constitutive
932 promoter localizing to the vascular tissues in primary roots. Scale bar: 100 µm.
933 (**d**) Quantification of cell death in sorbitol-treated root tips. Boxplots represent
934 the relative PI staining (sorbitol/control) for each genotype. Averages from five
935 independent biological replicates (n>31). Different letters represent significant
936 differences (p-value<0.05) in an ANOVA plus Tukey's HSD test. Boxplots
937 represent the median and interquartile range (IQR). Whiskers depict Q1-
938 1.5*IQR and Q3+1.5*IQR and points experimental observation.

939

940 **Figure 2. The BRL3 receptor promotes root hydrotropism responses.**
941 (**a**) Root curvature (hydrotropic response) in seven-day-old roots after 24 h of
942 sorbitol-induced osmotic stress (270 mM). Scale bar: 0.2 cm. (**b**) Discrete
943 distribution of root hydrotropic curvature angles in the different genotypes.

944 Lightest green depicts roots curved between 0º and 10º, light green between
945 10º and 20º, dark grey between 20º and 30º, and darkest green depicts roots
946 that have a curvature of more than 30º as indicated in the color legend. (**c**)
947 Continuous distribution of root curvature angles. Different letters indicate a
948 significant difference (p-value<0.05) in a one-way ANOVA test plus Tukey's
949 HSD test. Boxplot represent the median and interquartile range (IQR). Whiskers
950 depict Q1-1.5*IQR and Q3+1.5*IQR and points experimental observations. Data
951 from four independent biological replicates (n>50). (**d**) Stress traits matrix for all
952 physiological assays performed on the roots and shoots of WT, BR loss-of-
953 function mutants and *BRL3ox*. Root growth in control conditions is highlighted in
954 green. Color bar depicts values for scaled data.
955
956 **Figure 3. BRL3 overexpression confers drought tolerance.**
957 (**a**) From top to bottom, three-week-old plant rosette phenotypes of WT,
958 *brl1brl3, bak1*, *brl1brl3bak1*, *bri1, bri1brl1brl3, quad* and *BRL3ox* grown in well-
959 watered conditions (left column), after 12 days of drought stress (middle
960 column) and after 7 days of re-watering (right column). (**b**) Plant survival rates
961 after 7 days of re-watering. Averages of five independent biological replicates
962 +/- s.e.m. (n>140). Asterisk indicates a significant difference (p-value<0.05) in a
963 chi-squared test for survival ratios compared to WT. (**c**) Bar plot shows the days
964 needed to reach different percentages of the soil field capacity for each
965 genotype used in the study. **(d)** Relative water content (RWC) of mature
966 rosettes at 0% (field capacity), 50% and 70% soil water loss. **(e**) Photosynthesis
967 efficiency (µmol/m2*s) at different percentages of soil water loss. (**d, e**) Boxplot
968 represent the median and interquartile range (IQR). Whiskers depict Q1-

969 1.5*IQR and Q3+1.5*IQR and points experimental observations (n=6). Different
970 letters depict significant differences within each genotype in a one-way ANOVA
971 plus a Tukey's HSD test. (**f**) Schematic representation of BR signaling levels,
972 adult plant size and drought resistance. Loss-of-function mutants passively
973 avoid stress (drought avoidance), whereas plants with increased levels of BRL3
974 act actively to avoid drought stress (drought tolerance).
975
976 **Figure 4. BRL3 overexpression plants show a primed metabolic signature.**
977 (**a**) Metabolites differentially accumulated in *BRL3ox* (dark green) *or quad (*light
978 green) shoots relative to WT at basal conditions. (**b**) Metabolites differentially
979 accumulated in *BRL3ox* (dark green) *or quad (*light green) roots relative to WT
980 at basal conditions. (**a, b**) Boxplot represent the median and interquartile range
981 (IQR). Whiskers depict Q1-1.5*IQR and Q3+1.5*IQR and points experimental
982 observations (n=5). Asterisks denote statistical differences in a two-tailed t-test
983 (p-value < 0.05) for raw data comparisons *BRL3ox* vs WT (panel right side) or
984 *quad* (panel left side). (**c**) Metabolites following differential dynamics between
985 *BRL3ox* and WT shoots along the drought time course. (**d**) Metabolites
986 following differential dynamics between *BRL3ox* and WT roots along the
987 drought time course. (**c, d**) Heatmap represents the log2 ratio of *BRL3ox*/WT.
988 (**e-j**) Clustering of the dynamics of relative metabolite levels along the drought
989 time course in shoots and roots. Solid lines show the actual metabolic profile
990 (averages) of the representative metabolite for each cluster while dashed lines
991 represent the polynomial curve that best fit the profile. Statistical significance
992 was evaluated with the maSigPro package. (**e**) Metabolites following a linear
993 increase during drought in shoots include Glucose, Glucose-1P, *myo*-inositol,

994 and Sinapate. (**f**) Proline follows a steeper exponential increase in *BRL3ox*
995 shoots. (**g**) Metabolites following an exponential increase in *BRL3ox* shoots but
996 nearly a linear increase in WT include galactose, GABA, phenylalanine,
997 tyrosine, 2-methylmalate, lysine, isoleucine, leucine, nicotinate, uracil, and
998 tryptophan. (**h**) Metabolites following a steeper exponential increase in *BRL3ox*
999 roots include trehalose, sucrose, proline and raffinose. (**i**) Metabolites following
1000 a reduced linear increase until a certain maximum in *BRL3ox* roots include
1001 glycerate and malate. (**j**) Metabolites following an exponential increase in
1002 *BRL3ox* roots but a linear increase in WT include glucose, fructose, *myo*-
1003 inositol, galactose, and asparagine.
1004
1005 **Figure 5. Stress genes are constitutively activated in *BRL3ox* roots.**
1006 (**a**) Most representative GO categories enriched in *BRL3ox* roots from the
1007 upregulated genes at time 0 and after 5 days of drought (**b**) Deployment of
1008 genes within "Response to stress" (GO:0006950) term that are also annotated
1009 as responsive to water, salt, heat, cold, and light stress. Colors in the heatmap
1010 represent the log2 fold change of *BRL3ox* vs. WT roots in control conditions (C)
1011 or the differential drought response (log2(FC drought/CTRL in *BRL3ox*) –
1012 log2(FCdrought/CTRL in WT)) if the gene is affected by the interaction
1013 genotype*drought (Int.). Red color in the squared heatmaps on the right shows
1014 that the gene has been previously identified as a direct target of BES1 or BZR1
1015 transcription factors. (**c**) Most representative GO categories enriched in *BRL3ox*
1016 roots from the upregulated genes at time 0 and after 5 days of drought. (**d**) Most
1017 representative GO categories enriched among genes affected by the interaction
1018 genotype-drought. GO categories enriched in genes activated in *BRL3ox* under

1019 drought compared to WT (left column) in genes repressed in *BRL3ox* under
1020 drought compared to WT (right column). Color bars: –log of p-value (adjusted
1021 by Benjamini-Hochberg or non-adjusted).
1022
1023 **Figure 6. Enrichment of deregulated genes in *BRL3ox* root vasculature.**
1024 (**a**) Tissue enrichment for upregulated (red) or downregulated (blue) genes in
1025 control conditions. Bars trespassing the p-value threshold (0.05) were
1026 considered enriched in the dataset. (**b**) Tissue enrichment for genes affected by
1027 the interaction genotype*drought Bars trespassing the threshold p-value<0.05
1028 were considered enriched in the dataset. (**a-b**) Deregulated genes tissue
1029 enrichment. AGL42: Quiescent center, APL: Phloem + Companion cells,
1030 COBL9: Root hair cells, CORTEX: Cortex, GL2: Non-hair cells, J2661:
1031 Pericycle, JO121: Xylem pole pericycle, LRC: Lateral root cap, PET111:
1032 Columella, RM1000: Lateral root primordia, S17: Phloem pole pericycle, S18:
1033 Maturing Xylem, S32: Protophloem, S4: Developing xylem, SCR5: Endodermis,
1034 SUC2: Phloem. y-axes represent the negative logarithm of one-tailed Fisher's
1035 test. (**c**) Deregulated genes enriched in the Pericycle (J2261 marker). (**d**)
1036 Deregulated genes enriched in the Phloem Pole Pericycle (S17 marker). (**c,d**)
1037 Bars represent the log2 fold-change of *BRL3ox* vs. WT roots in control (black)
1038 or the difference of drought responses between *BRL3ox* and WT (FC
1039 drought/CTRL in *BRL3ox* – FC drought/CTRL in WT) in the lineal model (gray).
1040 Blue boxes highlight enzymes directly involved in the metabolism of deregulated
1041 metabolites.
1042
1043

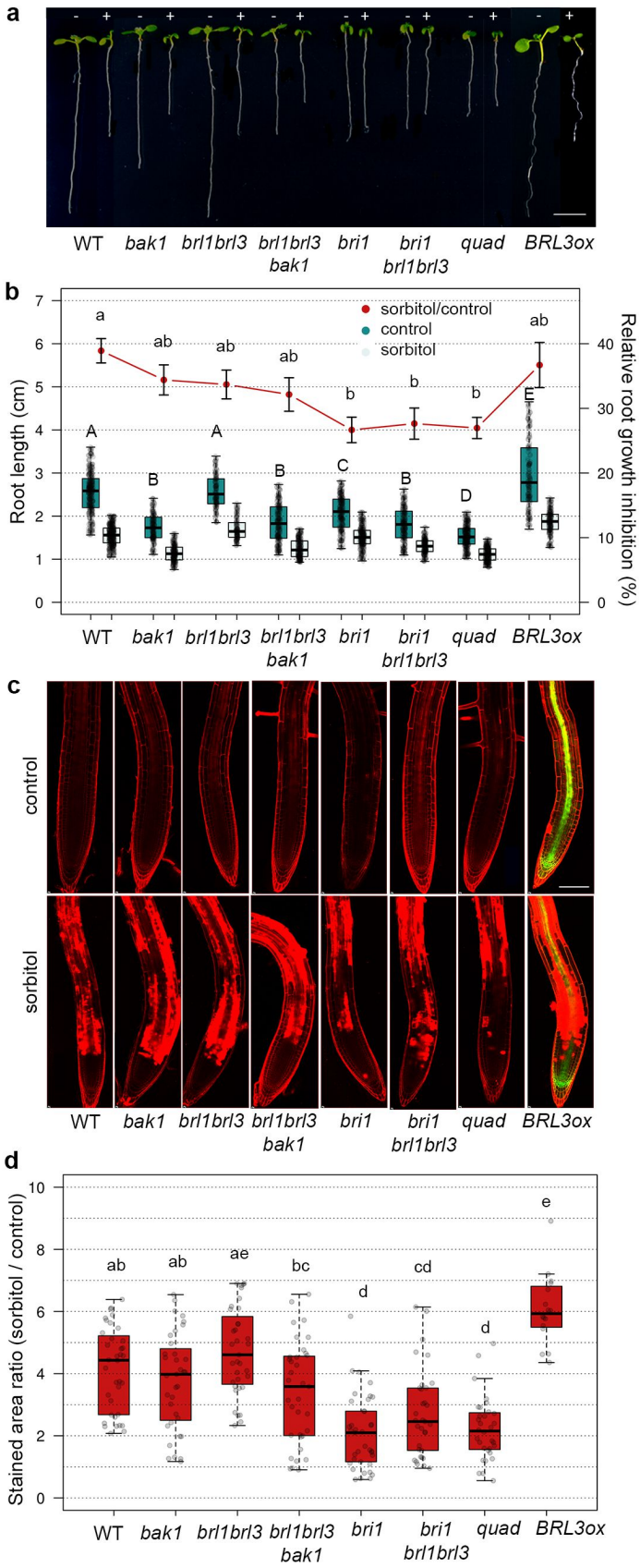

Figure 1. BR perception mutant roots are less sensitive to osmotic stress.

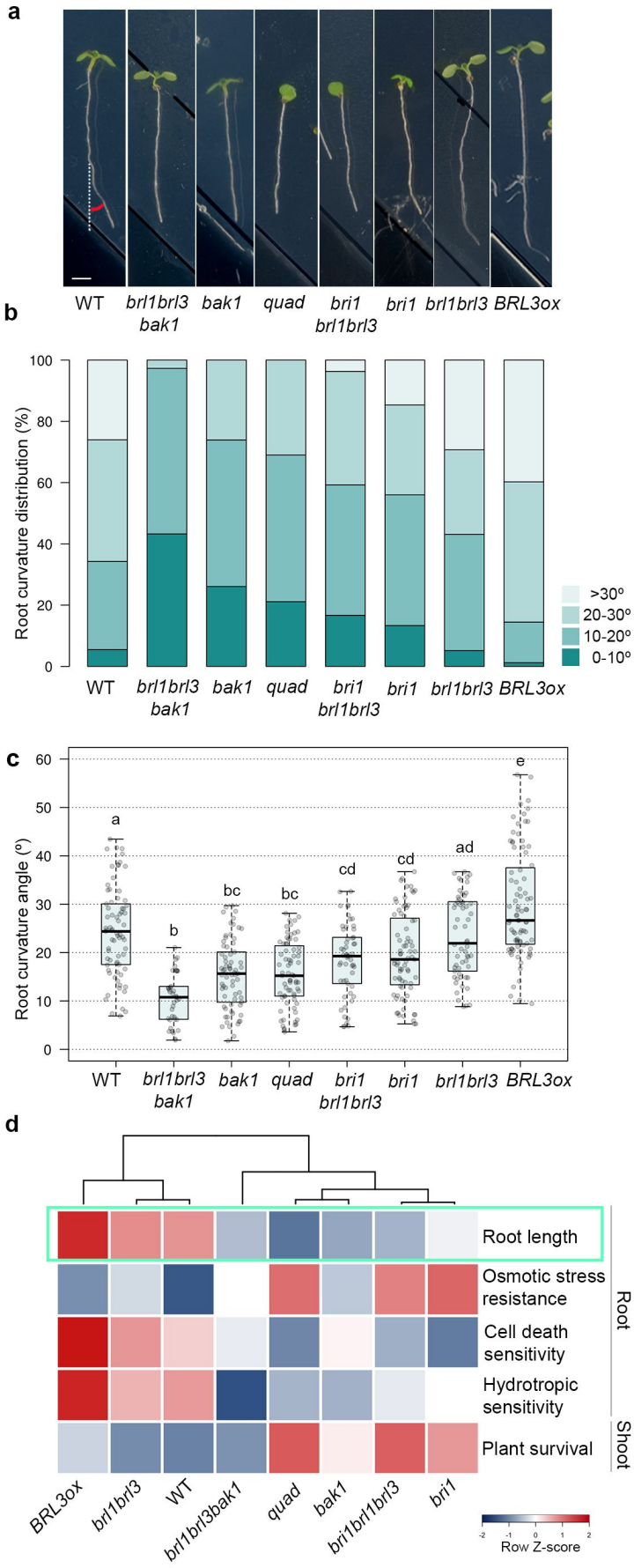

Figure 2. The BRL3 receptor promotes root hydrotropism responses

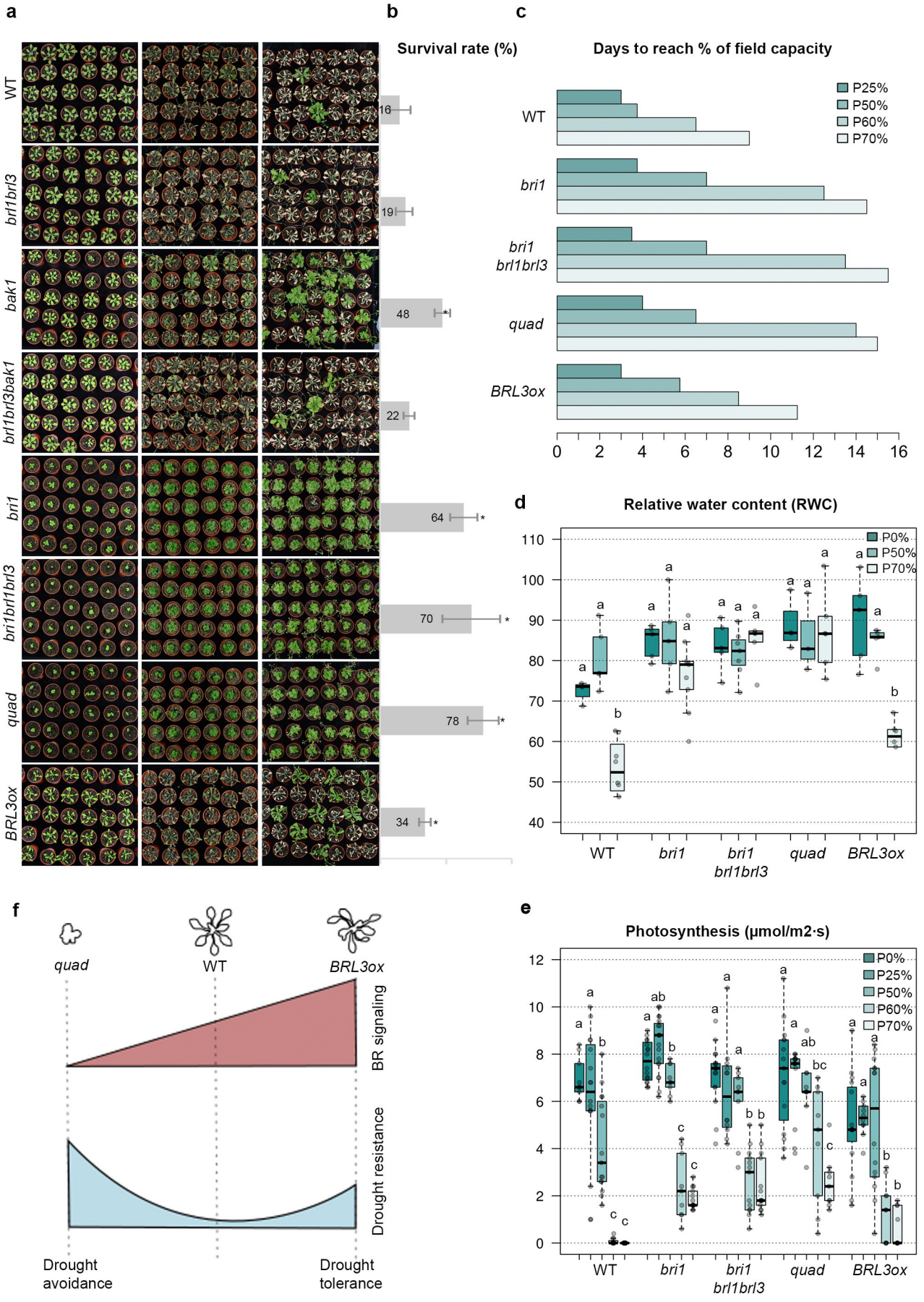

Figure 3. BRL3 overexpression confers drought tolerance.

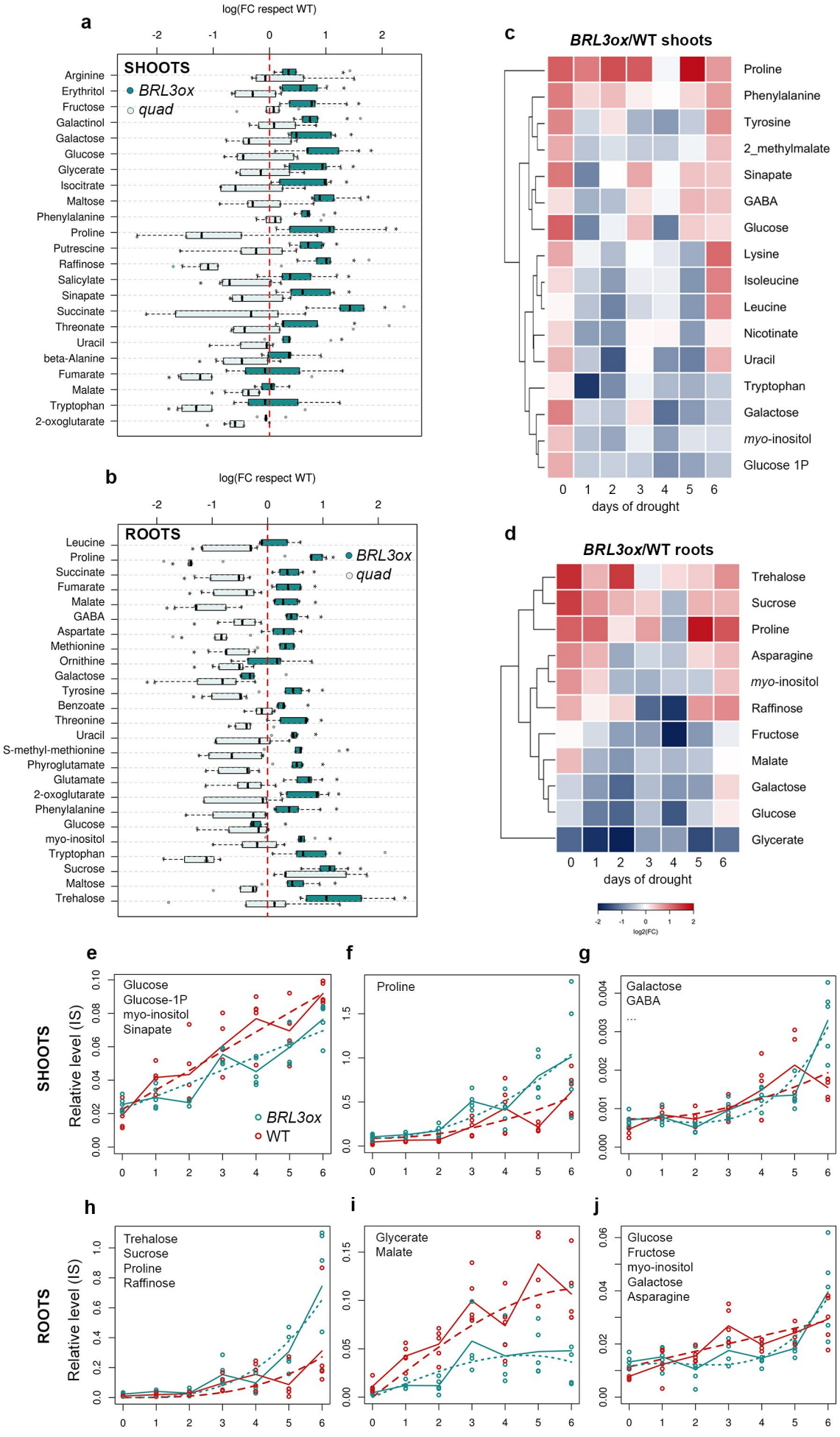

Figure 4. BRL3 overexpression plants show a primed metabolic signature

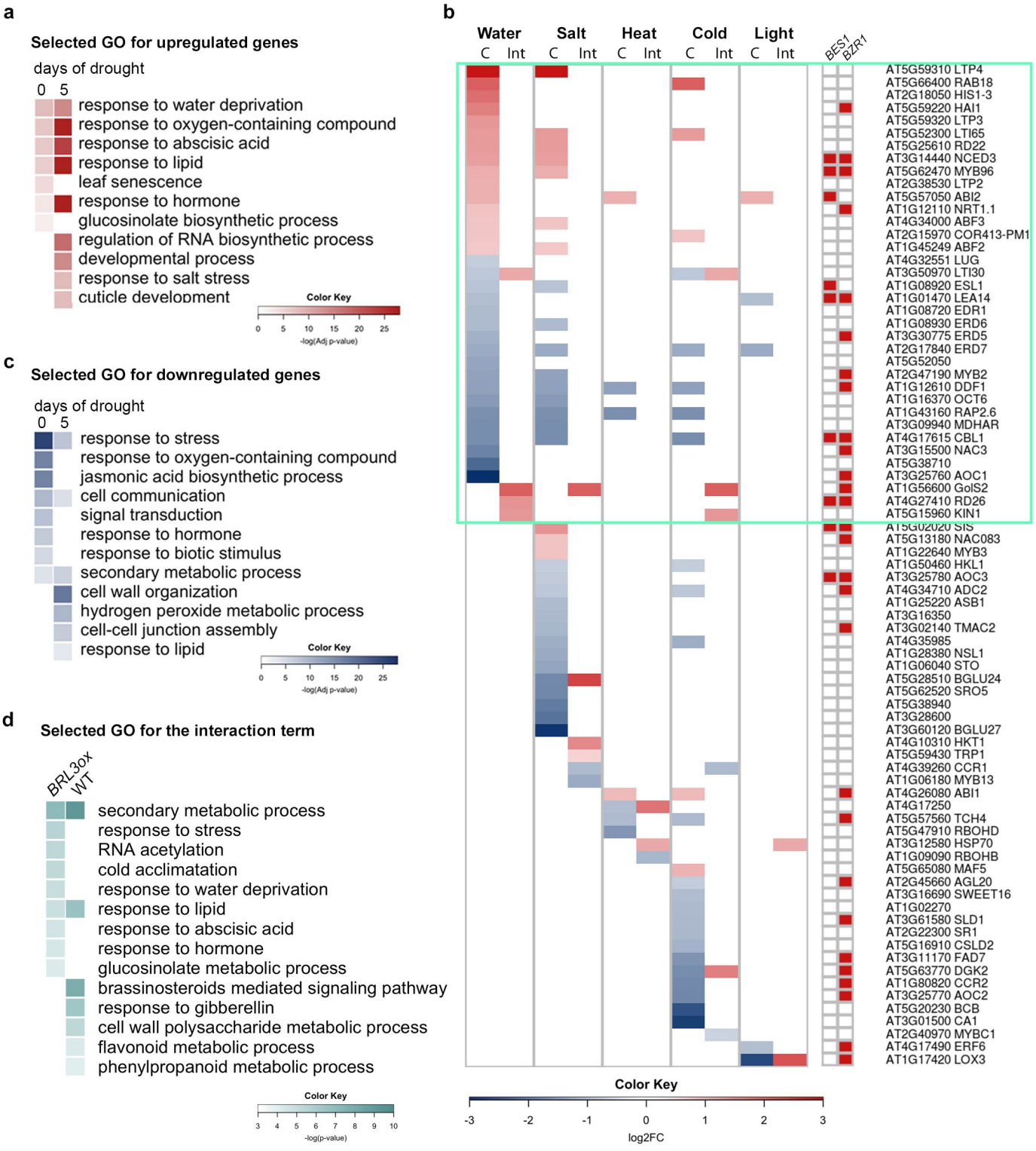

Figure 5. Stress genes are constitutively activated in *BRL3ox* roots.

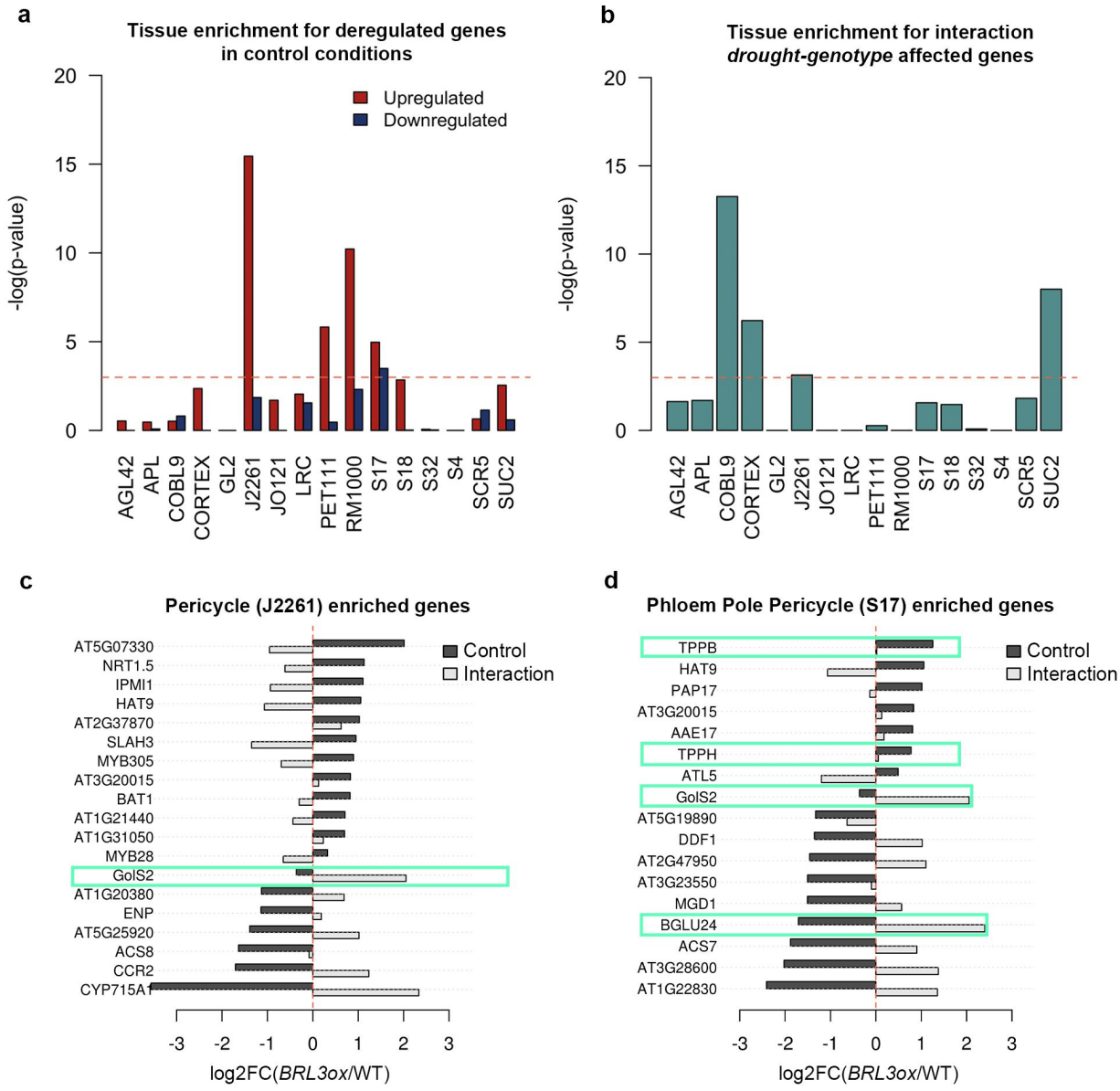

Figure 6. Enrichment of deregulated genes in *BRL3ox* root vasculature.